

Hybrid CO₂-Ti:sapphire laser with tunable pulse duration for mid-infrared-pump terahertz-probe spectroscopy

Matthias Budden,^{1, a)} Thomas Gebert,^{1, a)} and Andrea Cavalleri^{1, 2, b)}

¹⁾ *Max Planck Institute for the Structure and Dynamics of Matter, 22761 Hamburg, Germany*

²⁾ *Department of Physics, Clarendon Laboratory, University of Oxford, Oxford OX1 3PU, United Kingdom*

(Dated: 24 November 2020)

Ultrafast optical excitation with intense mid-infrared and terahertz pulses has emerged as a new tool to control materials dynamically. As most experiments are performed with femtosecond pulse excitation, typical lifetimes of most light-induced phenomena in solids are of only few picoseconds. Yet, many scientific applications require longer drive pulses and lifetimes. Here, we describe a mid-infrared pump – terahertz-probe setup based on a CO₂ laser seeded with 10.6 μm wavelength pulses from an optical parametric amplifier, itself pumped by a Ti:Al₂O₃ laser. The output of the seeded CO₂ laser produces high power pulses of nanosecond duration, which are synchronized to the femtosecond laser. Hence, these pulses can be tuned in pulse duration by slicing their front and back edges with semiconductor-plasma mirrors irradiated by replicas of the femtosecond seed laser pulses. Variable pulse lengths from 5 ps to 1.3 ns are achieved, and used in mid-infrared pump, terahertz-probe experiments with probe pulses generated and electro-optically sampled by the femtosecond laser.

INTRODUCTION

Intense mid-infrared (MIR) and terahertz light pulses are of strong interest for nonlinear ultrafast spectroscopy as well as for coherent manipulation of materials properties. Recently, such pulses have enabled the discovery of unconventional phenomena such as the formation of magnetic polarization in antiferromagnets¹, ferroelectricity in paraelectrics^{2,3}, new topological phases⁴, as well as non-equilibrium high T_c superconductivity in cuprates^{5,6} and molecular organic materials^{7–10}. Typically, these experiments are performed using sub-picosecond pulses with high peak electric field ($\sim 5 - 10$ MV/cm). The lifetime of the induced transient state is therefore often limited to a few picoseconds. In the pursuit of longer-lived, functionally relevant photo-induced states, there is an increasing demand for laser sources producing mid-infrared and terahertz pulses with tunable duration from hundreds of femtoseconds to hundreds of picoseconds¹⁰.

Laser sources based on narrow band gap semiconductors, such as IV-VI compounds (lead salts) and wavelength tunable quantum cascade lasers readily produce radiation in the mid-infrared region of the electromagnetic spectrum ($\sim 2.5 - 30$ μm wavelength). However, these sources often require cryogenic cooling¹¹, and their emitted power is not sufficient to reach sufficiently intense pulses, as field strengths in excess of few MV/cm are required for non-linear excitation of materials.

Typically, high peak power mid-infrared pulses are generated via optical parametric amplification and frequency mixing starting from ultra short light pulses generated by conventional solid state lasers (e.g. Ti:Al₂O₃ or Yb:YAG). This approach yields pulses with energies of 10 - 50 μJ and allows to reach MV/cm peak electric fields only for pulses with sub-picosecond durations. Although gas lasers based on CO ($\lambda = 5 - 6$ μm) and CO₂ ($\lambda = 9 - 11$ μm) can

^{a)}Co-first authors with equal contribution

^{b)}Electronic mail: andrea.cavalleri@mpsd.mpg.de

easily produce high energy mid-infrared pulses¹²⁻¹⁴, they are typically not mode-locked resulting in pulse-to-pulse time and intensity fluctuations that make pump-probe experiments with picosecond precision difficult.

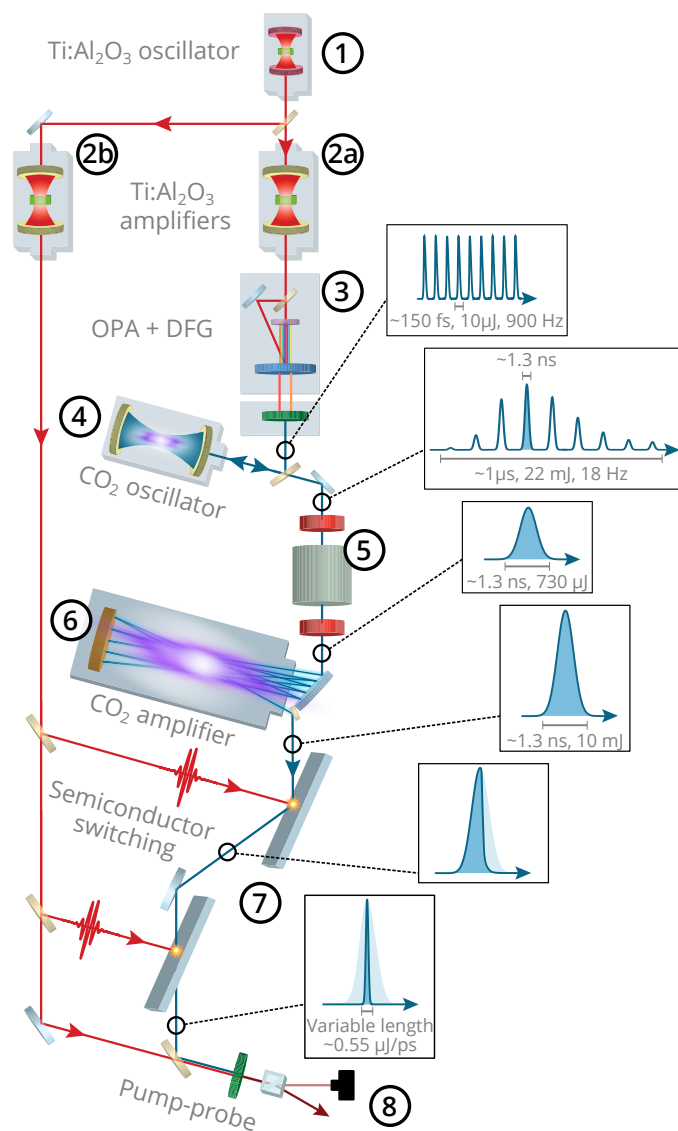


FIG. 1. Experimental setup for the generation of high power, pulse length tunable mid-infrared pulses (1) Ti:Al₂O₃ oscillator ($f = 80$ MHz, $\lambda = 800$ nm, $E = 6.25$ nJ), (2) Ti:Al₂O₃ amplifiers (a: $E = 5$ mJ, b: $E = 7$ mJ), (3) OPA and DFG ($\lambda = 10.6$ μ m) (4) Injection seeded CO₂ oscillator ($\lambda = 10.6$ μ m) (5) CdTe Pockels cell selects most intense pulse (6) CO₂ multipass amplifier (7) Semiconductor switching (8) Cross-correlation and pump-probe experiment.

Here we present a hybrid optical source based on a combination of ultrafast Ti:Al₂O₃ and CO₂ lasers to perform pump-probe measurements using intense MIR pulses with tunable duration. Figure 1 displays a schematic of the experimental setup. A CO₂ laser chain is seeded with radiation generated by an ultrafast optical parametric amplifier to generate mid-infrared pulses at 10.6 μ m that are optically synchronized to the Ti:Al₂O₃ source, enabling experiments with sub-picosecond time resolution.

GENERATION OF MODE-LOCKED MID-INFRARED PULSES WITH CO₂ LASERS

The gain spectrum of the CO₂ laser consists of multiple lines with a bandwidth of about 3.7 GHz and about 55 GHz spacing originating from the vibrational-rotational transitions in the laser gas (see Fig. 2b). This bandwidth is much larger than the typical spacing of cavity modes of about 100 MHz (see Fig. 2c) so that multiple longitudinal modes can be excited at the same time even if the gain is limited to a single rotational line (e.g. with a grating reflector). Figure 2a displays the typical single shot output of a commercial transversely excited CO₂ laser, revealing multi-mode operation arising from amplified spontaneous emission.

Whilst mode-locking techniques based on saturable absorbers, electro- or acousto-optic modulators facilitate the formation of reproducible high power output pulses^{15–17}, they are not well suited to synchronize the generated MIR pulses to a probe beam. This limitation can be overcome by externally seeding the CO₂ laser cavity, both as a means of active mode locking and to facilitate synchronization^{18,19}. For this purpose, we generated 150 fs long 10.6 μm wavelength pulses in a 1.5 mm thick GaSe crystal by difference frequency mixing of the signal (1490 nm) and idler (1730 nm) outputs of a home built optical parametric amplifier (OPA). The OPA was pumped with 3 mJ pulse energy, 100 fs long pulses from a commercial Ti:Al₂O₃ regenerative amplifier (see Fig. 1). A fraction of these femtosecond pulses (~60 pJ) was injected through the semi-transparent (R: 80%, T: 20%) front window into the cavity of the CO₂ laser. The bandwidth of the injected femtosecond pulses was spectrally filtered to match the narrower gain bandwidth of the CO₂ laser cavity (see Fig. 2b, c) by spatial selection of the first diffraction order of the intracavity grating reflector, which acted as a rear mirror only for the desired rotational line around 10.6 μm. The injection of these seed pulses induces an active mode locking resulting in a train of output pulses, synchronized to the femtosecond seed laser²⁰. A typical time-intensity trace of the seeded output of the CO₂ oscillator is shown in Fig. 3b (blue curve). The peak intensity of the pulse train was about one order of magnitude higher than in the non-seeded case (red curve) due to the phase locking of all longitudinal cavity modes induced by the seed. The single pulses in the train were ~1.3 ns long, limited by the available gain bandwidth, and showed intensity fluctuations of less than 1%. These residual fluctuations can be attributed

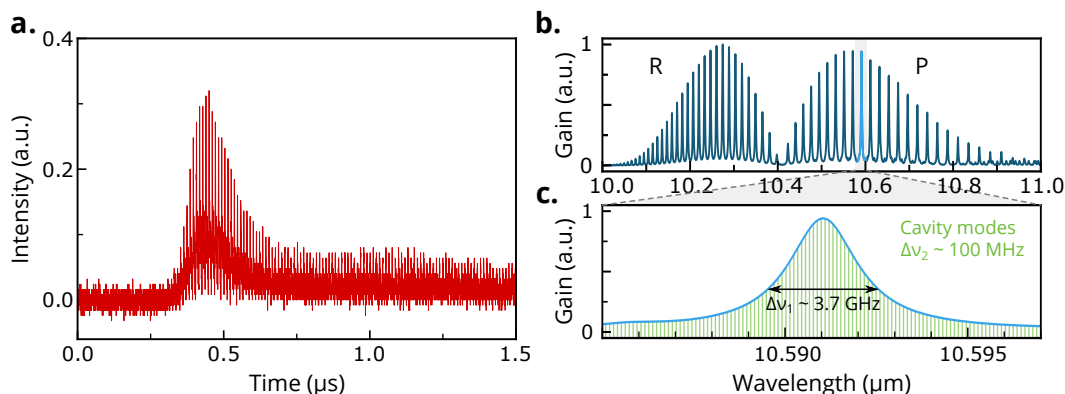


FIG. 2. Amplified spontaneous emission and multimode operation of the CO₂ laser oscillator. **a.** Time-intensity profile of the pulse emitted from a commercial CO₂ laser showing the superposition of several longitudinal modes. The most intense mode causes distinct spikes to appear every ~10 ns corresponding to the roundtrip time of the ~1.5 m cavity. The pulse has an envelope of a few microseconds. **b.** Calculated gain spectrum of molecular CO₂ at ambient pressure. Rotational transitions with a spacing of ~55 GHz form the R- and P-branches. A grating reflector within the cavity selects only one transition around 10.6 μm. **c.** Calculated gain spectrum of the selected rotational line compared to the frequency spacing of the longitudinal cavity modes. The ~3.7 GHz gain bandwidth is much wider than the 100 MHz spacing of the longitudinal cavity modes resulting in arbitrary excitation of multiple cavity modes when the laser is amplifying spontaneous emission.

to small temporal variations of the electrically triggered plasma build-up, which translated into a time jitter of the gain curve. For the specific laser used in this work, the optimal timing for seed injection was found to be ~ 700 ns after the plasma excitation is triggered. Under these conditions, the pulse build-up time was reduced by ~ 150 ns as compared to unseeded operation and the output intensity was highest.

The most intense pulse in the train was selected by a custom-built pulse picker based on the combination of a CdTe Pockels-cell (Fig. 1-5) and a wire-grid polarizer. To reach the required pulse energy for the envisioned experiments, this isolated pulse was further amplified from ~ 0.7 mJ to ~ 10 mJ in a subsequent CO₂ laser amplifier, built from a commercial laser that we modified to operate as a 10-pass amplifier (Fig. 1-6) at a repetition rate of 18 Hz.

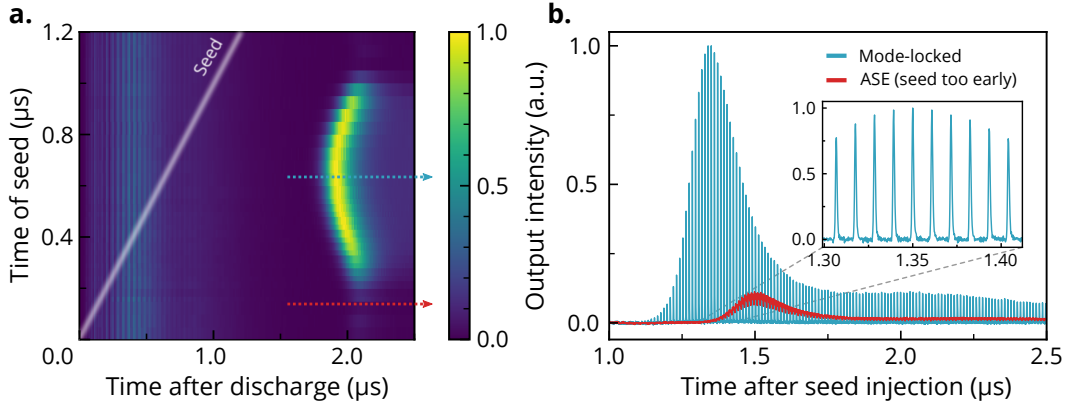


FIG. 3. CO₂ laser injection seeding **a.** Map of the measured CO₂ laser output traces vs. time of the injected seed pulse. The color indicates the output intensity. Both time axes are referenced to the trigger of the plasma discharge. The discharge leads to a stable electronic noise floor within the first microsecond after the trigger. The seed injection time is shown as a white line. The two dashed lines correspond to single time traces shown in **b.** **b.** Averaged output intensity time traces of the CO₂ laser are shown for the case of amplified spontaneous emission when the 100 fs long seed pulse is injected too early (red curve) as well as for optimal seeding (blue curve). The inset shows a section of a single-shot time trace of the seeded laser indicating perfect mode-locking.

MID-INFRARED PULSE DURATION CONTROL

Although a pressure or electric field (through the AC Stark effect) broadened spectral gain can support the amplification of picosecond CO₂ laser pulses, it requires either an amplifier with a gas cell pressurized at 10 – 15 bar^{21–23} or multi-stage preamplification for the generation of laser fields with intensities of more than 5 GW/cm²²⁴. As the mid-infrared pulses produced in our setup are inherently synchronized to a femtosecond near infrared source, another viable option for tailoring their pulse duration is the use of electron-hole plasmas in photoexcited semiconductors as ultrafast shutters. This technique, first described in detail in Ref.²⁵, has been applied in different laser systems for external pulse shortening^{23,26} as well as for the reflection of a single pulse out of a laser cavity^{27–29}.

In our implementation, shown schematically in Fig. 4a, the p-polarized mid-infrared laser pulse was transmitted through an optically flat semiconducting plate set at Brewster's angle to suppress any reflection in the unpumped state. A short near-infrared laser pulse, derived from the Ti:Al₂O₃ chain used to seed the CO₂ oscillator was used to excite a plasma of electron-hole pairs. Optical excitation made the semiconductor surface highly reflective for all frequencies lower than the electron-hole-density-dependent plasma frequency. After

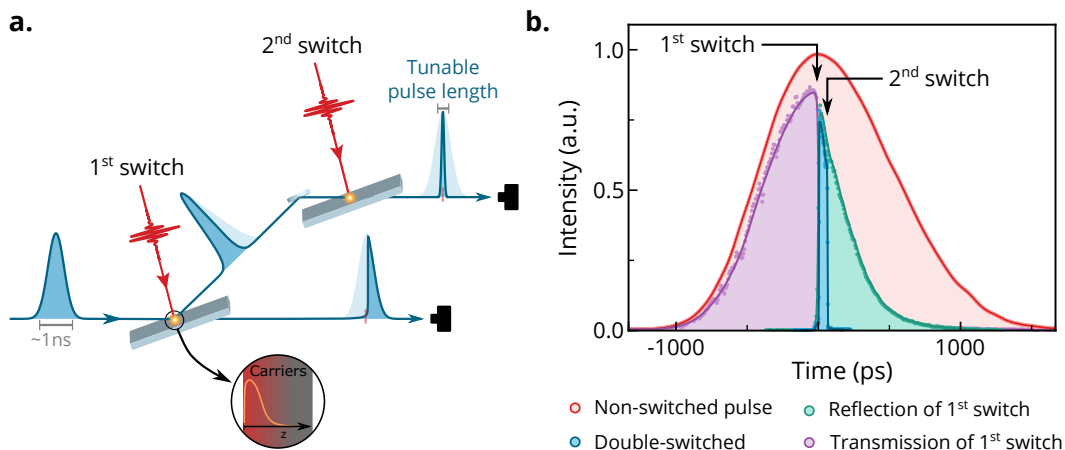


FIG. 4. Principle of semiconductor switching. **a.** Schematic of the setup for generation of continuously adjustable pulse lengths. The incoming MIR CO₂ laser pulse (blue) impinges on a semiconductor at Brewster's angle and its leading edge is fully transmitted. A second short NIR pulse (800 nm wavelength, ~ 100 fs duration, red) excites an electron-hole plasma at spatio-temporal overlap with the MIR pulse. Within few picoseconds, the carrier density rises, which renders the semiconductor highly reflective and slices the MIR pulse. A subsequent switch can cut the trailing edge so that precise pulse length tunability is possible by adjusting the optical delay between the two NIR slicing pulses. **b.** Cross correlation curves of the unswitched (red) CO₂ laser beam as well as for single transmissive (violet), single reflective (green) and double switched pulses (blue). Upon switching, the semiconductor reflectivity changes within less than 5 ps creating sharp edges in the pulse.

optical excitation, the critical carrier density for full reflection can be obtained from:

$$n_c^* = \frac{\epsilon_0 \epsilon_r m^* \omega_l^2}{e^2}, \quad (1)$$

where ω_l is the laser frequency and ϵ_0 , ϵ_r , m^* , and e denote the vacuum and semiconductor dielectric constants, the effective carrier mass and the electron charge, respectively. To create a reflective surface for CO₂ laser radiation at $10.6 \mu\text{m}$ wavelength, a carrier density in excess of $10^{18} - 10^{19} \text{ cm}^{-3}$ is needed depending on the type of semiconductor. Si, Ge, CdTe, and GaAs all feature high mid-infrared transparency and critical carrier densities that can be achieved with modest ($< 10 \text{ mJ/cm}^2$) excitation fluences.

The combination of a reflection and a transmission switching enabled the generation of short pulses of variable length that could be adjusted by appropriately delaying the control pulses. In order to compensate the optical path in the CO₂ lasers of ~ 400 m, the near-infrared excitation pulse for semiconductor switching was derived from a second Ti:Al₂O₃ amplifier seeded with a later pulse from the master oscillator (see Fig. 1). The remaining optical delay of ~ 2 m was compensated with an optical delay line to achieve accurate timing.

To perform pump-probe experiments using these pulses we required high switching efficiency, wide pulse length tuning range (10 ps to more than 500 ps), and a high background suppression of at least 1:1000. To achieve a high switching contrast, good mid-infrared transparency in the unexcited state and high reflectivity in the photoexcited state were required.

Figure 4b displays typical time-traces of the resulting $10.6 \mu\text{m}$ pulses before and after switching using silicon both as a reflection and transmission switch. These measurements were performed by cross-correlation of the mid-infrared generation in a 2 mm thick GaSe crystal. Different semiconductors feature distinct decay dynamics³⁰⁻³² of the electron-hole plasma. Figure 5a shows a comparison of the time-dependent $10.6 \mu\text{m}$ reflectivity of a single semiconductor switch made of silicon, germanium and cadmium telluride. These curves were

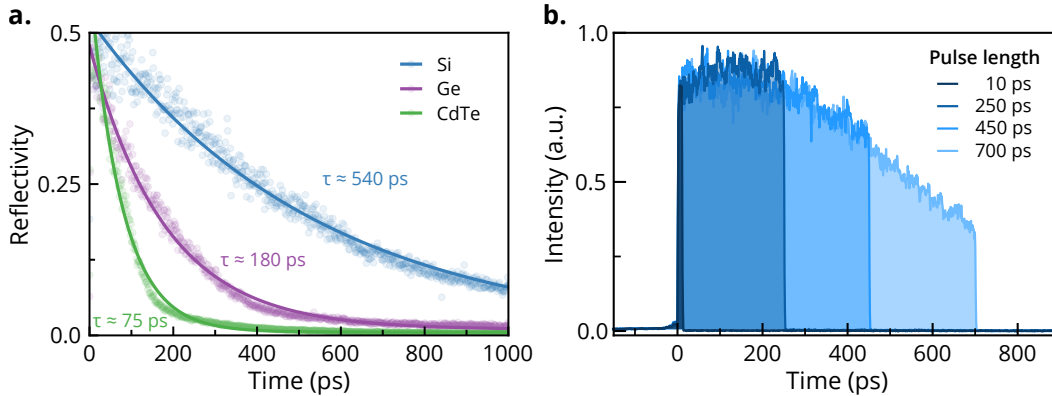


FIG. 5. Time profile of semiconductor plasma reflectivity and switched pulses **a.** The temporal evolution of the reflected fraction of the incoming pulse is shown for three different slicing materials. Note that the power of the 800 nm control beam was adjusted for every switch for maximum efficiency without damaging the material. **b.** Time profile of the intensity of the $10.6 \mu\text{m}$ pulses after slicing on two silicon wafers in reflection and transmission. The traces are a result of a cross-correlation measurement following the procedure described in the text.

extracted from cross-correlation measurements shown exemplarily in Fig. 4b by calculating the time dependent ratio of the reflected intensity from the semiconductor to the intensity of the unswitched beam. The decay rate of the reflectivity could be fitted by a single exponential decay in all the three cases and was found to be the longest in Si (550 ps) and the shortest in CdTe (75 ps).

When output pulses below 50 ps are desired, using CdTe as the first reflection switch provided the best background suppression ratio ($> 1000:1$) thanks to its fast reflectivity decay. The background suppression was measured through cross-correlation of the double sliced pulse shown in Fig. 5b by averaging over a time window of 50 ps on the pulse and 50 ps after the trailing edge of the pulse. On the other hand, for output pulse durations in excess of 50 ps, a Si reflection switch was preferred to maintain high reflectivity for a longer time. In this case, due to the large penetration depth of the near-infrared excitation pulse, thick plasma layers are formed so that transmission of the MIR radiation is negligible³⁰. This makes Si a good candidate also for the second switch, both for the generation of short and long pulses. As this switch is used to suppress the trailing edge of the pulse, it is most effective if the radiation is to be blocked for as long as possible after photoexcitation.

The pulse lengths of double sliced pulses obtained with two silicon switches could be tuned over a wide range from ~ 5 ps to ~ 1 ns whilst for durations up to 300 ps almost flat-top-intensity pulses were achieved (see time profiles in Fig. 5b). Although the minimum rise and fall time of the mid-infrared pulse is determined by the near infrared excitation pulse duration, in our setup the two pulses impinge on the semiconductors with a 13° non-collinear angle leading to a few picosecond temporal spread on the semiconductor surface. The damage threshold was found to be significantly material dependent being just above 5 mJ/cm^2 for Si, 3.9 mJ/cm^2 for CdTe, and 1.7 mJ/cm^2 for Ge. For fluence levels below damage threshold a maximum switching efficiency of 50% was achieved for all materials.

MIR-PUMP THZ-PROBE EXPERIMENT ON INSB

To demonstrate the applicability of the setup for pump-probe experiments with adjustable excitation pulse-lengths, we measured the time-resolved reflection of THz radiation from an InSb wafer excited with $10.6 \mu\text{m}$ pulses with durations varying between 5 ps and 100 ps (see Fig. 6). These pulses were generated using a CdTe reflection and a Si transmission switch and their time-intensity profile is shown in Fig. 6b. THz pulses with bandwidth from

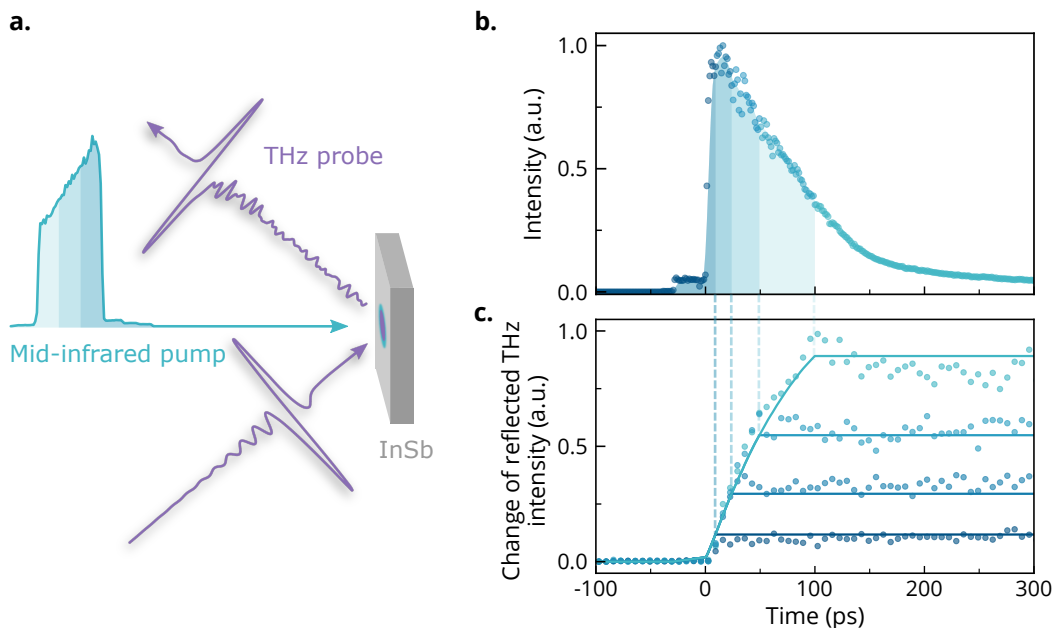


FIG. 6. Optical integrator on InSb **a.** Schematic of the experimental setup for pulse length tunable mid-infrared pump, THz probe spectroscopy **b.** Cross-correlation measurement of a $10.6\ \mu\text{m}$ laser pulse with $1.3\ \text{ns}$ pulse length that was reflection switched with $100\ \text{fs}$ long $800\ \text{nm}$ wavelength pulses on CdTe. The decay of the semiconductor reflectivity due to carrier diffusion results in the declining slope of the reflected pulse. The different shadings indicate the pulse shapes that remain when using a second transmission switch after $10\ \text{ps}$, $20\ \text{ps}$, $50\ \text{ps}$ and $100\ \text{ps}$. **c.** Measured change of reflected THz intensity of an InSb sample upon excitation with the pulses shown in **a.** (dots). Solid lines represent the calculated integral of the pulse intensity measurement from Fig. 6a up to the respective pulse duration of $10\ \text{ps}$, $20\ \text{ps}$, $50\ \text{ps}$ and $100\ \text{ps}$. The reflectivity change in InSb scales with the incident number of photons, not with the electric field.

$\sim 0.5\ \text{THz}$ to $\sim 3\ \text{THz}$ were generated in a commercial photoconductive antenna excited with $100\ \text{fs}$ long pulses at $800\ \text{nm}$ wavelength. These THz pulses were focused on the InSb sample, and their electric field was measured after reflection by means of electro-optic sampling in a $1\ \text{mm}$ thick (110)-cut ZnTe crystal.

Upon irradiation with the $10.6\ \mu\text{m}$ pump pulses, the reflected THz intensity (the square of the THz electric field) increased linearly with the integral of the pump pulse intensity cross-correlation measurements, which we determined to be linear with the number of pump photons. After the $10.6\ \mu\text{m}$ pump pulses hit the InSb wafer, the respective reflectivity levels stayed nearly constant for the observable measurement time of several hundred picoseconds. Therefore, the InSb response acts like an optical integrator of the pump photons.

In summary, we demonstrated a hybrid optical device that generates high-power mid-infrared pulses based on seeded CO_2 lasers, with tunable pulse durations achieved with two semiconductor-based plasma mirrors. This source allows the extension of ultrafast experiments from femtosecond drives to pulse durations of hundreds of picoseconds. As the mid infrared pulses were naturally synchronized in time to a femtosecond laser, this device made pump-probe experiments with sub-picosecond resolution possible.

FUNDING

The research leading to these results received funding from the European Research Council under the European Union's Seventh Framework Programme (FP7/2007-2013)/ERC Grant Agreement No. 319286 (QMAC). We acknowledge support from the Deutsche

Forschungsgemeinschaft (DFG) via the Cluster of Excellence ‘The Hamburg Centre for Ultra-fast Imaging’ (EXC 1074 – project ID 194651731).

ACKNOWLEDGEMENTS

We thank Michele Buzzi and Guido Meier for their help with manuscript preparation. Furthermore, we are grateful to Michael Volkmann for his technical assistance in the construction of the new optical apparatus presented in this work. We also acknowledge Toru Matsuyama, Boris Fiedler and Birger Höhling for their support with electronics and Jörg Harms for his help with graphics. Additionally, we thank Yannis Laplace for support in the early stage of the experimental design.

DISCLOSURES

The authors declare no conflicts of interest.

- ¹A. S. Disa, M. Fechner, T. F. Nova, B. Liu, M. Först, D. Prabhakaran, P. G. Radaelli, and A. Cavalleri, “Polarizing an antiferromagnet by optical engineering of the crystal field,” *Nature Physics* **16**, 1–5 (2020).
- ²X. Li, T. Qiu, J. Zhang, E. Baldini, J. Lu, A. M. Rappe, and K. A. Nelson, “Terahertz field-induced ferroelectricity in quantum paraelectric SrTiO₃,” *Science* **364**, 1079–1082 (2019).
- ³T. F. Nova, A. S. Disa, M. Fechner, and A. Cavalleri, “Metastable ferroelectricity in optically strained SrTiO₃,” *Science* **364**, 1075–1079 (2019).
- ⁴Y. H. Wang, H. Steinberg, P. Jarillo-Herrero, and N. Gedik, “Observation of floquet-bloch states on the surface of a topological insulator,” *Science* **342**, 453–457 (2013).
- ⁵D. Fausti, R. I. Tobey, N. Dean, S. Kaiser, A. Dienst, M. C. Hoffmann, S. Pyon, T. Takayama, H. Takagi, and A. Cavalleri, “Light-induced superconductivity in a stripe-ordered cuprate,” *Science* **331**, 189–191 (2011).
- ⁶W. Hu, S. Kaiser, D. Nicoletti, C. R. Hunt, I. Gierz, M. C. Hoffmann, M. Le Tacon, T. Loew, B. Keimer, and A. Cavalleri, “Optically enhanced coherent transport in YBa₂Cu₃O_{6.5} by ultrafast redistribution of interlayer coupling,” *Nature Materials* **13**, 705–711 (2014).
- ⁷M. Mitranò, A. Cantaluppi, D. Nicoletti, S. Kaiser, A. Perucchi, S. Lupi, P. Di Pietro, D. Pontiroli, M. Riccò, S. R. Clark, D. Jaksch, and A. Cavalleri, “Possible light-induced superconductivity in K₃C₆₀ at high temperature,” *Nature* **530**, 461–464 (2016).
- ⁸A. Cantaluppi, M. Buzzi, G. Jotzu, D. Nicoletti, M. Mitranò, D. Pontiroli, M. Riccò, A. Perucchi, P. Di Pietro, and A. Cavalleri, “Pressure tuning of light-induced superconductivity in K₃C₆₀,” *Nature Physics* **14**, 837–841 (2018).
- ⁹M. Buzzi, D. Nicoletti, M. Fechner, N. Tancogne-Dejean, M. A. Sentef, A. Georges, T. Biesner, E. Uykur, M. Dressel, A. Henderson, T. Siegrist, J. A. Schlueter, K. Miyagawa, K. Kanoda, M.-S. Nam, A. Ardavan, J. Coulthard, J. Tindall, F. Schlawin, D. Jaksch, and A. Cavalleri, “Photomolecular high-temperature superconductivity,” *Physical Review X* **10**, 031028 (2020).
- ¹⁰M. Budden, T. Gebert, M. Buzzi, G. Jotzu, E. Wang, T. Matsuyama, G. Meier, Y. Laplace, D. Pontiroli, M. Riccò, F. Schlawin, D. Jaksch, and A. Cavalleri, “Evidence for metastable photo-induced superconductivity in K₃C₆₀,” arXiv:2002.12835 [cond-mat] (2020), arXiv:2002.12835 [cond-mat].
- ¹¹M. Tacke, “Lead–salt lasers,” *Philosophical Transactions of the Royal Society of London. Series A: Mathematical, Physical and Engineering Sciences* **359**, 547–566 (2001).
- ¹²M. Endo and R. F. Walter, eds., *Gas Lasers*, Optical Science and Engineering No. 121 (CRC/Taylor & Francis, Boca Raton, 2007).
- ¹³G. A. Mesriats, *Pulsed Power* (Kluwer Academic/Plenum Publishers, New York, 2005).
- ¹⁴A. J. Beaulieu, “Transversely excited atmospheric pressure CO₂ lasers,” *Applied Physics Letters* **16**, 504–505 (1970).
- ¹⁵A. F. Gibson, M. F. Kimmitt, and B. Norris, “Generation of bandwidth-limited pulses from a TEA CO₂ laser using p-type germanium,” *Applied Physics Letters* **24**, 306–307 (1974).
- ¹⁶A. Nurmikko, T. A. DeTemple, and S. E. Schwarz, “Single-mode operation and mode locking of high-pressure CO₂ lasers by means of saturable absorbers,” *Applied Physics Letters* **18**, 130–132 (1971).
- ¹⁷O. R. Wood and S. E. Schwarz, “Passive q-switching of a CO₂ laser,” *Applied Physics Letters* **11**, 88–89 (1967).
- ¹⁸G. L. Bourdet, R. A. Muller, G. M. Mullot, and J. Y. Vinet, “Active mode locking of a high pressure CW waveguide CO₂ laser,” *Applied Physics B* **44**, 107–110 (1987).
- ¹⁹T. J. Bridges and P. K. Cheo, “Spontaneous self-pulsing and cavity dumping in a CO₂ laser with electro-optic q-switching,” *Applied Physics Letters* **14**, 262–264 (1969).

- ²⁰M. Babzien, I. V. Pogorelsky, and M. Polanskiy, "Solid-state seeding of a high power picosecond carbon dioxide laser," in *Advanced Accelerator Concepts 2016: 16th Advanced Accelerator Concepts Workshop* (San Jose, CA, USA, 2016) p. 110001.
- ²¹B. Patel, "Collision broadening of high pressure CO and CO₂ laser transitions," *Physics Letters A* **45**, 137–138 (1973).
- ²²A. J. Alcock and A. C. Walker, "Generation and detection of 150-psec mode-locked pulses from a multi-atmosphere CO₂ laser," *Applied Physics Letters* **25**, 299–301 (1974).
- ²³P. Corkum, "Amplification of picosecond 10 μm pulses in multiatmosphere CO₂ lasers," *IEEE Journal of Quantum Electronics* **21**, 216–232 (1985).
- ²⁴D. Haberberger, S. Tochitsky, and C. Joshi, "Fifteen terawatt picosecond CO₂ laser system," *Optics Express* **18**, 17865–17875 (2010).
- ²⁵A. J. Alcock, P. B. Corkum, and D. J. James, "A fast scalable switching technique for high-power CO₂ laser radiation," *Applied Physics Letters* **27**, 680–682 (1975).
- ²⁶S. A. Jamison and A. V. Nurmikko, "Generation of picosecond pulses of variable duration at 10.6 μm ," *Applied Physics Letters* **33**, 598–600 (1978).
- ²⁷V. V. Apollonov, P. B. Corkum, and R. S. Taylor, "Selection of high-power nanosecond pulses from large-aperture CO₂ oscillators," *Applied Physics Letters* **35**, 147–149 (1979).
- ²⁸R. E. M. de Bekker, L. M. Claessen, and P. Wyder, "Generation of very short far-infrared pulses by cavity dumping a molecular gas laser," *Journal of Applied Physics* **68**, 3729–3731 (1990).
- ²⁹S. Marchetti, M. Martinelli, R. Simili, M. Giorgi, and R. Fantoni, "Controlled dumping of pulses of laser radiation ranging from MIR to the MM by means of optical semiconductor switching," *Applied Physics B* **72**, 927–930 (2001).
- ³⁰C. Rolland and P. B. Corkum, "Generation of 130-fsec midinfrared pulses," *Journal of the Optical Society of America B* **3**, 1625–1629 (1986).
- ³¹A. Y. Elezzabi, J. Meyer, M. K. Hughes, and S. R. Johnson, "Generation of 1-ps infrared pulses at 10.6 μm by use of low-temperature-grown GaAs as an optical semiconductor switch," *Optics Letters* **19**, 898–900 (1994).
- ³²A. Y. Elezzabi, *Ultrafast Switching of CO₂ Laser Pulses by Optically-Induced Plasma Reflection in Semiconductors*, Ph.D. thesis, Department of Physics, University of British Columbia (1995).